Supplementary Material

Evolution of Graphene Nanoribbons under Low-voltage Electron Irradiation

Wenpeng Zhu[1], Hongtao Wang[2*] and Wei Yang[2,1*]

[1] *AML, Department of Engineering Mechanics, Tsinghua University, Beijing 100084, China*

[2] *Institute of Applied Mechanics, Zhejiang University, Hangzhou 310027, China*

[*] To whom correspondence should be addressed. E-mail address: htw@zju.edu.cn and yangw@zju.edu.cn

Detailed implementation method for Rutherford scattering model

Fig. S1 shows the atomic model for MD simulations. The irradiation zone has a length of 80 Å between two thermostats. Atomic displacements record the major effects induced by e-beam irradiation. As compared to the MD time step of 1 fs, the collision effect is replaced by a transient energy transfer from electron to carbon nucleus. MD simulations capture the subsequent atomic motion due to interatomic collisions and thermal migration within the time scales from 10^{-13} s to 10^{-11} s.

The incoming electrons have uniform intensity on the projection plane A'-A" (Fig. S2) and the subsequent energy transfer is calculated according to the Rutherford scattering model. The displacement rate is estimated to be $p = \sigma \times j$ with σ being the scattering cross-section and j the beam intensity. The differential cross-section is given as:[1]

$$\frac{\mathrm{d}\sigma}{\mathrm{d}\Omega} = \left(\frac{Ze^2}{16\pi\varepsilon_0 E} \right)^2 \sin^{-4}\frac{\theta}{2}. \qquad \text{(S1)}$$

The parameters in the above equation are listed below:

$\frac{\mathrm{d}\sigma}{\mathrm{d}\Omega}$: The Rutherford differential scattering cross-section per solid angle

θ: The electron scattering angle

Z: Atomic number of the target nucleus

E (= 60 keV): The electron energy

e: Electron charge

ε_0: Vacuum permittivity

The total cross-section can thus be calculated as:

$$\sigma = \int_{\theta_0}^{\pi} \frac{\mathrm{d}\sigma}{\mathrm{d}\Omega} 2\pi \sin\theta \mathrm{d}\theta \tag{S2}$$

where θ_0 is the screening angle (with E being in keV):[2]

$$\theta_0 = 0.117 \frac{Z^{1/3}}{E^{1/2}}. \tag{S3}$$

For a single collision event, the differential scattering cross-section $\mathrm{d}\sigma$ can be derived as a function of the electron scattering angle θ (as from (S2))

$$\begin{aligned} \mathrm{d}\sigma &= \frac{\mathrm{d}\sigma}{\mathrm{d}\Omega} 2\pi \sin\theta \mathrm{d}\theta \\ &= 2\pi \left(\frac{Ze^2}{16\pi\varepsilon_0 E} \right)^2 \sin^{-4}\frac{\theta}{2} \sin\theta \mathrm{d}\theta \end{aligned}. \tag{S4}$$

According to the Rutherford model, the differential cross-section can also be expressed by the impact parameter b:

$$\mathrm{d}\sigma = \pi \mathrm{d}\left(b^2\right) = -2\pi \left(\frac{Ze^2}{16\pi\varepsilon_0 E} \right)^2 \sin\theta \sin^{-4}\frac{\theta}{2} \mathrm{d}\theta \tag{S5}$$

$$\Rightarrow \mathrm{d}\left(b^2\right) = -2 \left(\frac{Ze^2}{16\pi\varepsilon_0 E} \right)^2 \sin\theta \sin^{-4}\frac{\theta}{2} \mathrm{d}\theta. \tag{S6}$$

The negative sign is added to the equation to ensure that increasing the offset b decreases the electron scattering angle θ. For the case of elastic scattering, the relation $2\theta + \varphi = \pi$ is established due to the conservation of the total kinetic energy and the total momentum. Accordingly,

$$\mathrm{d}\left(b^2\right) = -8 \left(\frac{Ze^2}{16\pi\varepsilon_0 E} \right)^2 \cos^{-4}\varphi \mathrm{d}\left(\cos\varphi\right). \tag{S7}$$

Integrating equation (S7) with the initial condition

$$\sigma \to 0 \Leftrightarrow b \to 0, \theta \to \pi \Leftrightarrow \varphi \to 0 \Leftrightarrow \cos\varphi \to 1 \tag{S8}$$

one arrives at

$$b = \frac{Ze^2}{8\pi\varepsilon_0 E}\tan\varphi\,. \tag{S9}$$

Therefore, the deflection angle φ is given by:

$$\varphi = \begin{cases} \arctan\left(\dfrac{8\pi\varepsilon_0 E}{Ze^2}b\right) & b \le b_{\max} \\ \dfrac{\pi}{2} & b \ge b_{\max} \end{cases} \tag{S10}$$

with $b_{\max} = \dfrac{Ze^2}{8\pi\varepsilon_0 E}\cot\left(\dfrac{\theta_0}{2}\right)$.

The transferred energy T is given by[3]

$$T(\varphi) = T_{\max}\cos^2\varphi \tag{S11}$$

The e-beam irradiation is carried out with the incidence of one electron per nm^2 in every 100 fs. The high intensity is equal to 1.6×10^8 A/cm^2, which exhibits approximately 10^6 orders of magnitude larger than the current density of 100 A/cm^2 used in our experiments, so as to accelerate the edge evolution of GNRs. To verify the rationality of the acceleration method, the etching rates are quantified for GNRs with different intensities. The numbers of ejected atoms are shown to be linear with the current density and the modeling time. From high to low, the ejection rates for various GNRs are ordered as hybrid, zigzag and armchair before final rupture.

Post annealing processes and temperature effects

The thermally activated process is addressed by post annealing at an elevated temperature (2000 K). The irradiated GNRs were taken as the initial configurations as well as the reference for the projection displacement. Fig. S7 shows that the high temperature annealing removed most of the atomic rings by thermally activated edge reconstruction and relaxed local distortion by restoring the hexagonal lattice. Long-distance migration was not found, which might attribute to the reactive nature of edges. Ideal zigzag and armchair edges are thermally stable at 2000 K and no transformation was identified between the two. High temperature reconstruction only occurs on the defective edge and results in small roughness.

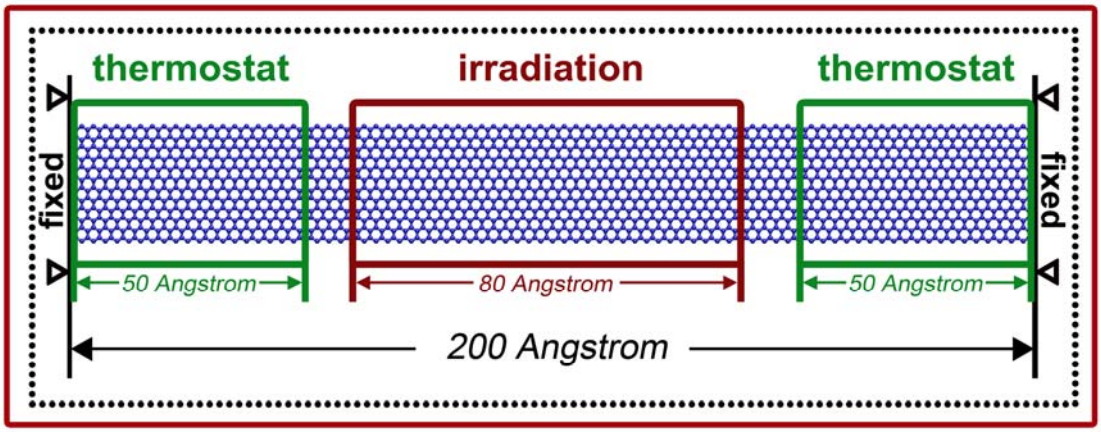

Fig. S1. Schematic of a 200 Å GNR with loading and constraint conditions set up in MD simulations. The two ends are fixed. The region in a red solid line is the irradiation zone that covers 80 Å span in the middle. The regions within green solid lines are thermostat zones having the length of 50 Å. The escape boundary is marked by the dot line. Any atoms ejected out will be removed from the simulation system.

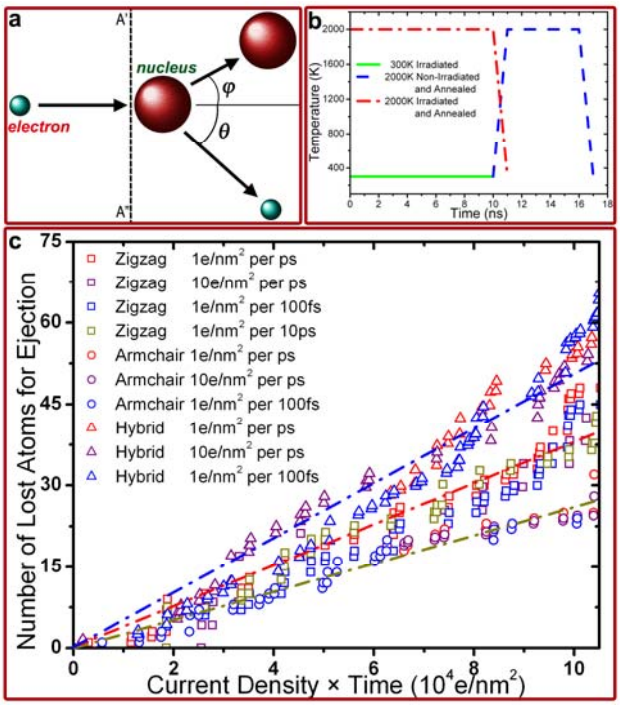

Fig. S2. (a) Schematic of an electron-nucleus collision model, adapted from Ref. 3. The incoming electrons have a uniform probability on the projection plane A'-A" toward the nucleus. (b) The temperature profiles in different simulations. The green solid line: a 10 ns irradiation at 300 K; The red dash dot line: a 10ns irradiation at 2000 K followed by a 1 ns cooling to 300 K; The blue solid line: a 7 ns quenching process of 2000 K without irradiation for the post-irradiated GNRs. (c) The numbers of ejected atoms as a function of electron exposure for different GNRs under varieties of irradiation intensities. The red, yellow and blue dash dot lines indicate the slopes of the zigzag, armchair and hybrid GNRs, respectively.

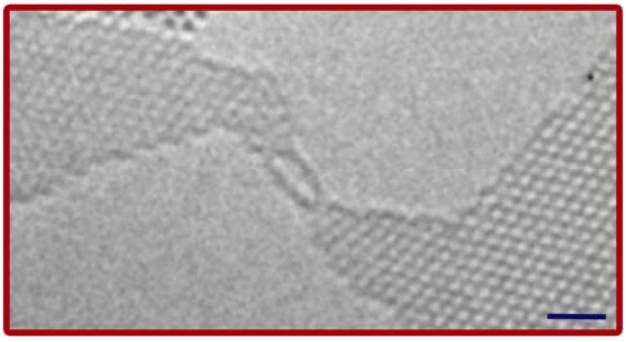

Fig. S3. Formation of a double mono-atomic chain from the ultrathin strip of GNR. Scale bar: 1 nm.

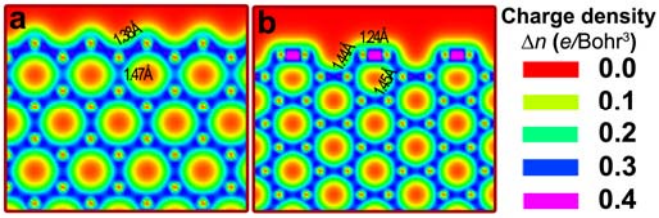

Fig. S4. The charge density distribution for the (a) zigzag and (b) armchair GNRs calculated by DFT. The lengths of the bonds located near the edges are labeled to confirm the bonding strengths.

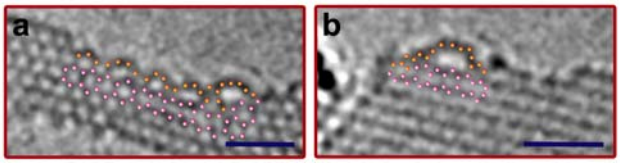

Fig. S5. Typical defect structures (polygon combination (a) and atomic chain (b)) observed by TEM at the zigzag edge under electron irradiation. The local atoms are highlighted by yellow dots. Scale bar: 1 nm.

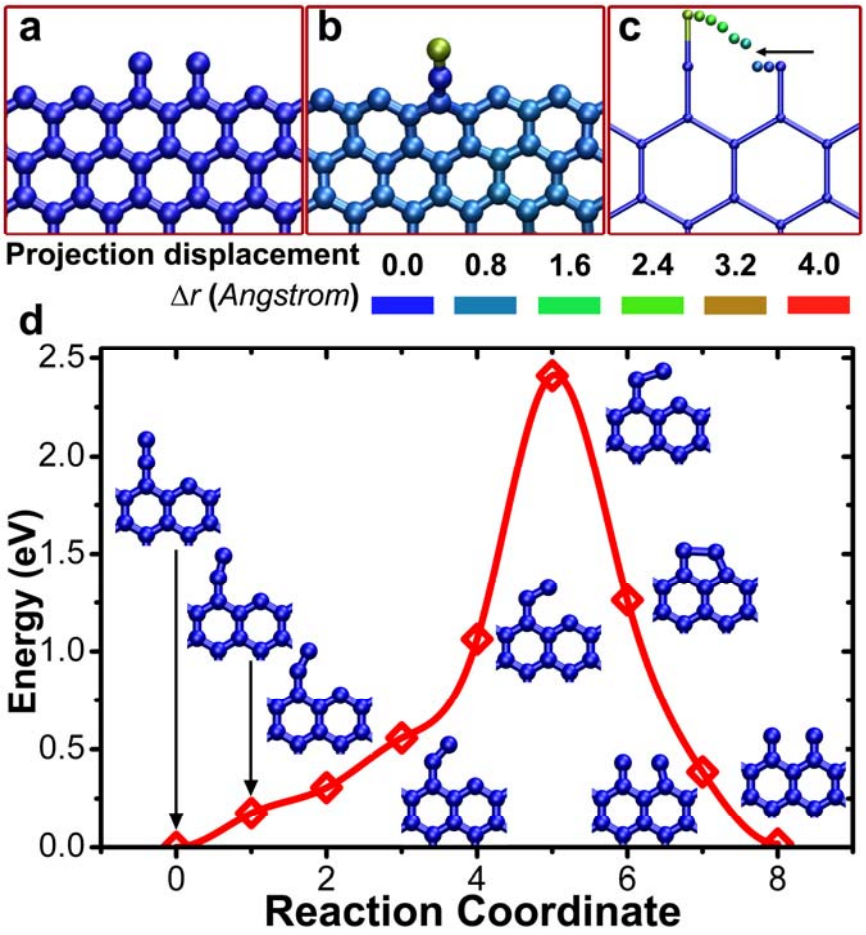

Fig. S6. Dangling atom migration along the edge. (a-b) Two successive snapshots with an interval of 10 ps. The right atom jumped onto a nearby dangling atom, forming a suspended nano-rod; (c) Migration path resolved by NEB method. A jumping process is identified by the discontinuity in the trace (indicated by an arrow). Atoms and bonds in (a-c) are colored by their projection displacements. (d) Energy profile that shows an energy barrier of 2.4 eV.

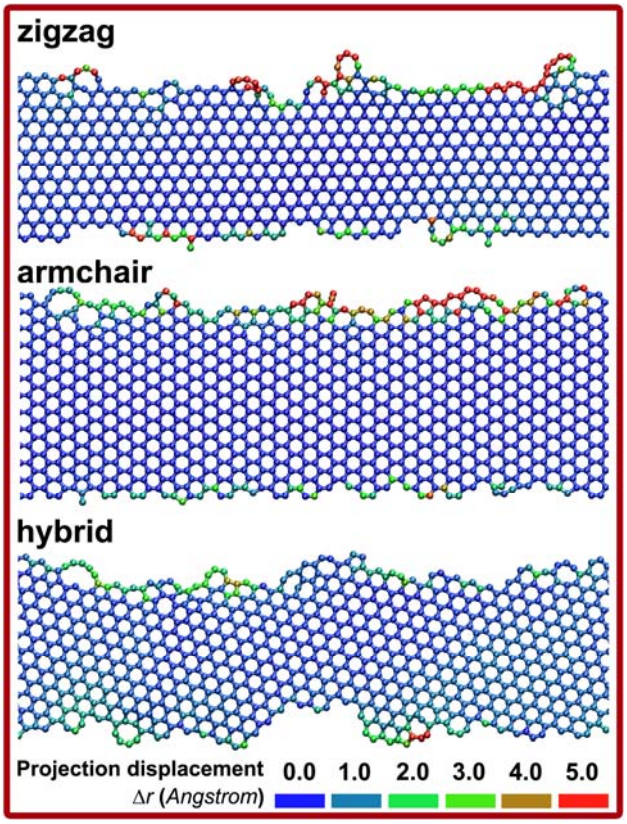

Fig. S7. Three irradiated GNRs are post-annealed at 2000K: (a) zigzag; (b) armchair and (c) hybrid edges.

Supplementary references

1. H. Kohl and L. Reimer, *Transmission Electron Microscopy: Physics of Image Formation*, Springer, New York, 2008.
2. D. B. Williams and C. B. Carter, *Transmission Electron Microscopy*, Springer, New York, 2007.
3. F. Banhart, *Rep. Prog. Phys.*, 1999, **62**, 1181.